Materials Research. 2022; 25:e20220008
DOI: https://doi.org/10.1590/1980-5373-MR-2022-0008

Tribological Behaviors Analysis of Synthesized Chromel Composite

***B. Mohmed Fazil*[a]*, *P. Suresh*[b]**

[a]*Sethu Institute of Technology, Department of Mechanical Engineering, 626115, Virudhunagar, India.*
[b]*Muthayammal Engineering College, Department of Mechanical Engineering, 637408, Rasipuram, India.*

Received: January 09, 2022; Accepted: February 01, 2022

This paper makes an investigation on the synthesis of tantalum carbide (TaC_x) based chromel composites and their tribological behaviour using pin on disc under various load conditions. The reinforced chromel alloy with TaC_x was prepared at the rate of 0, 3 and 6 wt.% of TaC using stir casting route. The wear resistance of composites was found to improve with the increase in weight percentage of TaC. The wear properties of Chromel-TaC_x composite were enhanced due to the presence of 6% TaC. The wear worn out surface of chromel composite was studied through microstructures. The optimal process factors and their effect on responses have been analyzed through Response Surface Methodology (RSM) and Analysis of Variance (ANOVA).

Keywords*: Chromel, Tantalum carbide, EDX, Worn surface morphology, Response surface methodology.*

1. Introduction

In recent days, nickel based chromium alloys are playing an essential role in metal industries. The combination of chromium with other alloys offers better substance properties. Nickel based chromium alloys were used in automotive industry, aero engines and nuclear reactors[1]. Chromel alloy was generally used as thermocouple. Chromel (K-type) thermocouple was applied to determine the outlet temperature[2]. Tungsten-copper and iron based chromel alloy were effectively utilized for temperature applications[3]. In direct contact type heat exchanger, chromel thermocouple was used to find the water temperature at the bottom of heat exchanger to withstand corrosion[4]. Tantalum carbide (TaCx) was used to enrich the carbon content of the material and also to strengthen the interfacial alloying elements through different compositions. The mechanical behaviors were also gradually improved[5]. As a result, different applications were suggested, including thermal heat insulation and vehicle wear-resistant liners. High volume fraction of tantalum carbide was applied for the improvement of fracture toughness and tensile strength[6]. The different compounds of tantalum carbide rich phases were used in alloy such as TaC, Ta_6C_5, Ta_4C_3 and Ta_2C[7]. Due to superior properties like high hardness, melting point, wear resistance and chemical stability, TaCx was observed to have a great effect on the substance properties[8]. The substance properties of MMC play a major role in the selection of material for any applications and processes. The three types of manufacturing process are (i) liquid state (ii) solid state, and (iii) solid-liquid[9]. Among these processes, liquid state process was found to be more economical. Stir casting was an example of liquid state processing technique. The advantages of using this process are better homogeneous material, cheap and uniform distribution of reinforcement particles. By using computer simulation, the effect of the stirrer velocity on the flow of material and possible distribution of reinforcement particles in the molten matrix yield improved material structure[10].

Reinforcements such as oxides, carbides, borides and nitrides with matrix usually minimize the wear of Al alloy[11]. The wear was increased due to the penetration of reinforcement material into the matrix and the forceful removal of debris material[12]. The wear rate was minimized due to the addition of reinforcement particles to the alloy and it was concluded that load was the top most factors to affect the wear rate[13]. AA 6082-T6 composite that was synthesized by reinforcing with an assortment of silicon and boron carbides using a stir casting process, subjected to a sliding wear test. Load, sliding speed, reinforcement percentage and sliding distance were selected as control factors. Variance analysis showed that the wear increases with an increase of sliding distance and load. However, a decrease in wear was observed with an increase in reinforcement or sliding speed[14]. Sliding wear test was performed on electroless Ni-P coating to investigate the wear behaviour and the test revealed that load and time have a major effect on two-way interaction[15]. An attempt to minimize the wear rate of Al/AlB_2 composites by employing L_9 Taguchi orthogonal array was done by considering the control factors of dry sliding wear behavior[16]. In recent times, Design of experiments was the most realistic statistical approach which was used in many fields for process control, design optimization and product performance prediction. The influence of input constraints on dry sliding wear behavior of SiC and graphite particles based reinforced aluminum composites were analyzed by carrying out L_{27} experiments under Taguchi DOE method. Among other factors, sliding distance was found to be the most significant factor[17].The experiments were performed to obtain the wear data in accordance with the experimental design of array. In particular, the impact of process factors

*e-mail: mohmedfazilmech@gmail.com

on the wear and frictional force performance characteristics in dry conditions were analyzed. The optimization was carried out for multiple quality characteristics by using grey relational analysis. The results of the wear analysis showed that a load of 20 N, 7 wt. % SiC and sliding distance of 1.046 m generated less wear[18]. An investigation was done to determine the influence of chromium on high manganese steel under different wear conditions. The study concluded that the addition of Cr yielded an increase in wear resistance, hardness and hardenability. High manganese steels alloyed with chromium displayed superior wear resistance[19].

The chromel composite was considered as the work material for this experiment due to its admirable properties and application. The present investigation describes the synthesis of tantalum carbide based chromel composite and their tribological behaviour under various load conditions. The optimal process factors and their effect of contribution have been analyzed through RSM and ANOVA.

2. Methodology

2.1. Wear experimentation

The Chromel –TaCx composite samples (0, 3 & 6% weight fraction) were subjected to dry sliding wear investigation on a pin-on-disc tribometer. The disc was made out of EN-31 steel of 62HRC with the structural dimensions of 100mm diameter and 10mm thickness. Cast samples were machined to form cylindrical pins of 10mm diameter and height 40mm as per ASTM G-99-95 standards[20]. By using acetone, the contact surface of the pin-disc was properly polished to minimize the errors. The specimens were finely polished by using emery sheets of 200, 400, 600, 800 and 1200 grit followed by 2000 grit in order to ensure the absence of debris. Then the polished surface is again cleaned with acetone so that oil particles or greasy particles would be removed. Three numbers of replicas carried out for each tribological condition. The applied load (10-30N), sliding distance (500-1500m) and weight percentage (0-6%) were used to evaluate the wear and frictional force. Totally 27 numbers of planned experiments were developed using Taguchi approach[21]. The chemical elements of chromel composite are presented in Table 1 while the wear experimental layout is shown in Table 2. The wear resistant of chromel composite was applied in bearings, drag liners and shaft.

2.2. Response Surface Modeling

Modeling and analyzing of engineering problems were performed by applying RSM technique which comprises of statistics and mathematical methods through different variables. It also measures the correlation between the control factors and the response factors. The advantages of RSM method were the reduction of the operating cost and the process variation. In addition, the RSM procedure comprises of experimental design for adequate and dependable quantity of the response and also forms an empirical model in obtaining the optimal set of experimental parameters. MINITAB Software was employed for the optimization using RSM. The general form of statistic equation was shown in Equation 1.

$$Y = f\left(x_1, x_2, x_3, x_4, \ldots\ldots, x_n\right) \quad (1)$$

Where, x_1, x_2, x_3, x_4 and x_n are the input process variables. Y is the outcome and x_1, x_2, x_3, and x4 are the quantitative variables. k_1, k_2, k_3 and k_4 represent the linear effects of x_1, x_2, x_3, x_4 respectively, k_{11}, k_{22}, k_{33} and k_{44} represent the quadratic effects of x_1, x_2, x_3, x_4. k_{12}, k_{13}, k_{14}, k_{23}, k_{24} and k_{34} represent the linear-by-linear interaction between x_1 and x_2, x1 and x_3, x1 and x_4, x_2 and x_3, x_2 and x_4, x_3 and x_4, respectively. This design fits well over defined design space. The response with respect to input factors was derived through RSM as shown in Equation 2.

$$Y = \begin{pmatrix} k_1 + k_1x_1 + k_2x_2 + k_3x_3 + k_4x_4 + k_{11}x_1^2 + k_{22}x_2^2 + k_{33}x_3^2 + k_{44}x_4^2 + \\ k_{12}x_1x_2 + k_{13}x_1x_3 + k_{14}x_1x_4 + k_{23}x_2x_3 + k_{24}x_2x_4 + k_{34}x_3x_4 \end{pmatrix} \quad (2)$$

The predicted responses were plotted and the responses were connected to obtain surface known as response surface plot. Variance analysis was used to confirm the experiment as well as to determine the contribution of the factors towards responses.

3. Result and Discussion

3.1. Material preparation

Chromel alloy was reinforced with 0, 3 and 6 wt % TaC through stir casting technique. One kg of chromel alloy was heated at the rate of 50°C/ 5 minutes up to 1400°C. The reinforcement particle of TaCx was preheated before adding with matrix. Once the matrix attained the molten state, reinforcement particles were added in graphite crucible. The molten matrix was stirred through stirrer attachment. The homogenous mixture was attained through double stirrer mechanism. The stirring was done (30 minutes) to mix the matrix and the reinforcement thoroughly to achieve the isotropic property. The slurry of the composite was poured into the preheated steel mould. The microstructure, composition and distribution of particle were shown in Figure 1a-c. The particle distribution on the surface of the material was clearly observed from the SEM image. Nickel was the major alloying element in chromel composite. The effect of different reinforcement particles and stir casting factors were investigated in Al composite[22]. The wear resistance increases with increase of load. The sliding velocity yield less effect on wear rate[23,24]. Nano hardness and wear rate was improved on silicon carbide based copper composite[25]. The investigation of multiple reinforcements and their effects were studied in aluminium composite[26]. The investigation of wear rate and bonding strength was conducted on composite coating with lamellar structure[27].

Table 1. Chemical elements of chromel composite.

S.No	Elements	Wt.%
1	Ni	89.01
2	Cr	09.43
3	Ta	01.10
4	C	00.46

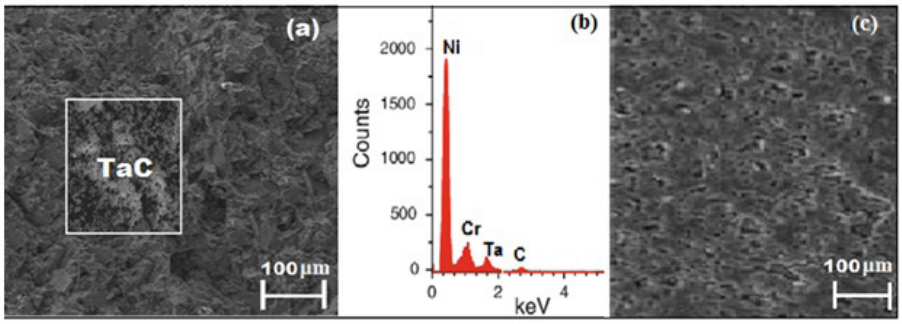

Figure 1. (a) SEM image and (b) EDAX image of chromel composite (c) Distribution of particles.

Table 2. Experimental layout.

Exp. No.	Input Factors			Responses	
	P (N)	SD (m)	W (wt.%)	Wear (µm)	FF (N)
1	10	500	0	67.3	4.30
2	10	500	3	52.6	6.16
3	10	500	6	40.8	5.12
4	10	1000	0	77.8	5.32
5	10	1000	3	54.7	5.24
6	10	1000	6	42.5	5.82
7	10	1500	0	75.2	6.42
8	10	1500	3	70.5	6.24
9	10	1500	6	51.6	6.12
10	20	500	0	82.8	9.82
11	20	500	3	56.8	10.44
12	20	500	6	45.06	12.22
13	20	1000	0	87.65	14.2
14	20	1000	3	59.3	9.82
15	20	1000	6	63.3	12.12
16	20	1500	0	97.9	12.2
17	20	1500	3	89.5	10.92
18	20	1500	6	73.08	13.82
19	30	500	0	90.5	14.32
20	30	500	3	67.1	14.98
21	30	500	6	61.1	14.82
22	30	1000	0	92.6	17.64
23	30	1000	3	65.3	16.86
24	30	1000	6	61.8	17.92
25	30	1500	0	109.7	18.82
26	30	1500	3	99.5	19.88
27	30	1500	6	94.5	18.86

3.2. Dry sliding wear of Chromel-TaC composite

The objective of the present investigation was to find the wear (µm) and frictional force (N) for Chromel-TaC composites using Response Surface Methodology (RSM). For better performance, the outcomes were considered as lower level. The obtained data for the two responses are presented in Table 2. These data were used to develop empirical RSM model in order to predict the output.

Figure 2 a-d shows the contour plot analysis for various input constraints. From Figure 2a, it is evident that wear loss was low for sliding distance range 500m to 1000m. Irrespective of the sliding distance, frictional force was less than 10N for applied load of 15N. It was not advisable to choose the applied load of more than 20N as well as sliding distance of more than 750m as shown in Figure 2b. Figure 2c shows that the unreinforced alloy exhibit more loss of material due to wear for all the combination of sliding distances. Figure 2d also revealed the same phenomenon as observed in Figure 2c where unreinforced alloy was subjected to high frictional force of 17.5N at 1000N.

The correlation between input factors and output factors were shown in Figure 2a-d. The correlation between load,

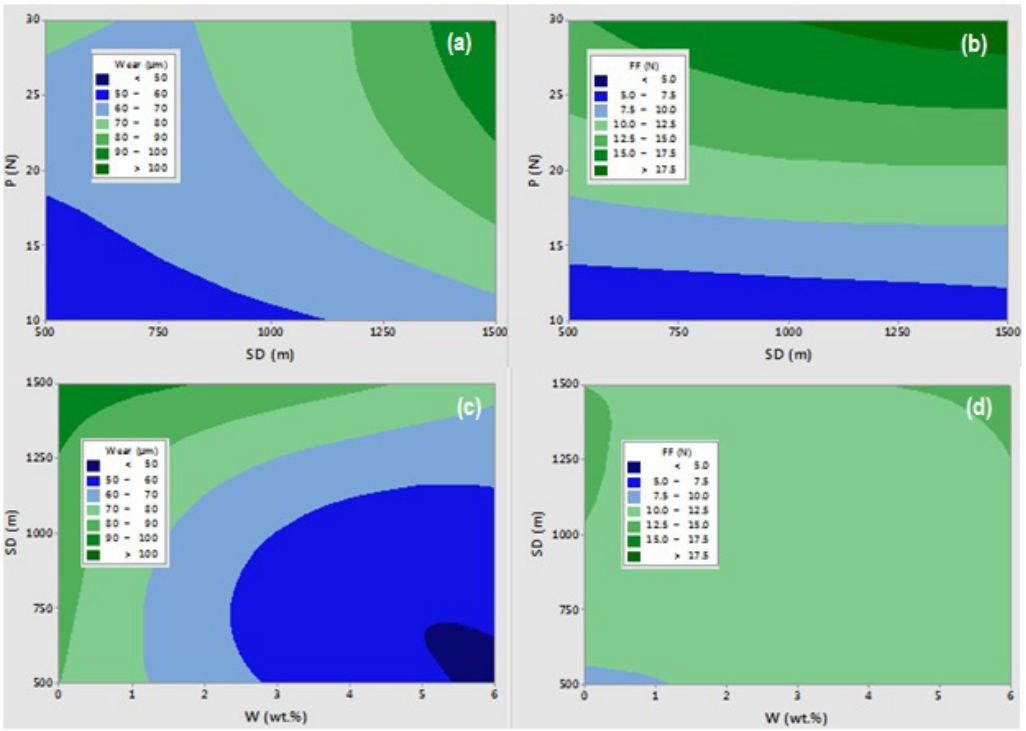

Figure 2. Correlation between (a) Load, SD and Wear (b) Load, SD and FF (c) SD, Wt % and Wear(d) SD, Wt % and FF.

SD and wear are shown in 2(a). The correlation between load, SD and FF are shown in 2(b). From 2(a) and 2(b) the wear and frictional force were highly increased at a load of 30N and SD of 1500m. The wear and frictional force were decreased at a load of 10N and SD of 500m. The correlation between SD, Wt % and wear are shown in Figure 2c. From 2(c) the wear was highly increased at wt % of 2 and SD of 1500 m. The correlation between SD, Wt % and FF are shown in 2(d). The low level of wear was attained at wt % of 1 and SD of 500 m.

3.3. Empirical model for wear and friction force

The empirical model, based on RSM for both wear as well as friction force, was presented in Equation 3 and Equation 4 respectively.

$$Wear = 79.3 + 1.06C2 - 0.0506C3 - 9.94C4 - 0.0198C2*C2 + 0.000026C3*C3 + 0.522C4*C4 + 0.000807C2*C3 + 0.0278C2*C4 + 0.00167C3*C4 \quad (3)$$

$$Friction\ Force = -5.22 + 1.0331C2 + 0.00158C3 + 0.557C4 - 0.01710C2*C2 - 0.0000032C3*C3 - 0.0734C4*C4 + 0.000050C2*C3 + 0.00300C2*C4 - 0.000108C3*C4 \quad (4)$$

Where, C2, C3 and C4 represent the respective input process factors.

The mathematical equation was developed based on square interaction effect. Applied load was the significant parameter in deciding the wear as per the developed Equation 3. The square interaction effect of applied load and sliding distance was most prevalent among other interactions. From Equation 4, it was clear that applied load was the vital in deciding friction force followed by interaction effect of applied load and weight percentage of reinforcement. Wear was increased with increase of contact pressure.

3.4. ANOVA for wear

Variance analysis was the statistical method used to assess the contributory importance of input factors towards output parameters. Since P-value was estimated at less than 0.05 for the three input parameters, these input parameters have some contribution towards output parameters. ANOVA results for wear are given in Table 3. The weight of the reinforcement got a vital role in affecting the response, followed by applied load and sliding speed. The contribution of weight %, applied load, and sliding distance are 42.58%, 27.06%, and 30.35% respectively as shown in Table 3. But interaction effect between parameters was not significant when compared to individual parameter. The validity was confirmed by R square value which is above 90% and it's shown in Equation 5.

$$R^2 Value = 95.2\%,\ adjusted\ R^2 = 93.5\%,\ predicted\ R^2 = 92.7\% \quad (5)$$

3.5. ANOVA for friction force

Variance analysis result for friction force is illustrated in Table 4. From the table, it can be seen that the applied load gives the largest effect on output followed by the sliding speed. Further, it can be noticed that the weight percentage of reinforcement has a negligible contribution in affecting

Table 3. Factor contribution of wear.

Source	DF	Adj SS	Adj MS	F-Value	P-Value	% of Contribution
Model	9	8685.58	965.06	27.94	< 0.005	
Linear	3	8003.21	2667.74	77.25	< 0.005	
Applied Load (C2)	1	2429.05	2429.05	70.33	< 0.005	30.35%
Sliding speed (C3)	1	2165.26	2165.26	62.7	< 0.005	27.06%
Wt.% (C4)	1	3408.9	3408.9	98.71	< 0.005	42.58%
Square	3	403.72	134.57	3.9	0.027	
C2*C2	1	23.58	23.58	0.68	0.42	
C3*C3	1	247.64	247.64	7.17	0.016	
C4*C4	1	132.51	132.51	3.84	0.067	
2-Way Interaction	3	278.65	92.88	2.69	0.079	
C2*C3	1	195.21	195.21	5.65	0.029	
C2*C4	1	8.33	8.33	0.24	0.63	
C3*C4	1	75.1	75.1	2.17	0.159	
Error	17	587.1	34.54			
Total	26	9272.68				

Table 4. Factor contribution of frictional force.

Source	DF	Adj SS	Adj MS	F-Value	P-Value	% of Contribution
Model	9	343.172	38.13	123.27	0.01	
Linear	3	321.854	107.285	346.83	0.03	
Applied Load (C2)	1	299.782	299.782	969.13	0.12	93.6
Sliding speed (C3)	1	21.303	21.303	68.87	0.011	
Wt.% (C4)	1	0.769	0.769	2.49	0.133	
Square	3	20.158	6.719	21.72	0.15	
C2*C2	1	17.542	17.542	56.71	0.06	
C3*C3	1	0.001	0.001	0	0.966	
C4*C4	1	2.615	2.615	8.45	0.01	
2-Way I	3	1.16	0.387	1.25	0.323	
C2*C3	1	0.749	0.749	2.42	0.138	
C2*C4	1	0.097	0.097	0.31	0.582	
C3*C4	1	0.314	0.314	1.01	0.328	
Error	17	5.259	0.309			
Total	26	348.431				

the response. The contribution of apR^2 Value = 96.1%, adjusted R^2 = 94.3%, predicted R^2=97.6%plied load and sliding distance are 93.3% and 6.6% respectively and shown in Table 4. The experimental validity was also confirmed by R square value which is above 90% and its shown in Equation 6.

$$R^2 Value = 96.1\ \%,\ adjusted\ R^2 = 94.3\%,\ predicted\ R^2 = 97.6\% \quad (6)$$

3.6. Worn surface morphology of Chromel-TaC composites

Figure 3 shows the worn surface morphology of (a) Chromel – 6 wt.% TaC at 30N (b) Chromel – 3 wt.% TaC at 30N, and (c) Chromel – 0 wt.% TaC at 30N at higher magnification.

The SEM images of the surface of the synthesized composites, after wear investigation, are presented in Figures 3a to 3c.

Figure 3a (stable state condition, applied load 30N; sliding distance of 1000m) shows the sliding direction and formation of wear debris on the rubbed surface of the Chromel – 6 wt.% TaC composites. Formation of debris was appeared due to the adhesion of TaC particle on the chromel alloy. Addition of 6% TaC improve the material at both high load and sliding velocity conditions. Figure 3b shows the worn out surface of SEM that indicates ploughing of material, which results in more removal of material. This occurs due to enormous plastic deformation and subsurface cracking[28]. As a result of ploughing, more pullout of material takes place. Figure 3c shows the formation of grooves, due to the transformation of nucleation crack into the fracture[29]. The wear rate of the composite depends on the amount of reinforcement particles[30]. The optimal coefficient of friction and grain refinement was analyzed in magnesium alloy[31]. The tribological behaviors were enhanced through laser treatment of the material surface[32].

Unreinforced alloy exhibit lesser wear resistance which resulted in more material removal due to wear. Thus deep groove was formed as shown in Figure 3c.

4. Optimal Solution

A developed the "desirability technique function" that can be commonly used in industrial sectors for multiple concurrent optimizations[33]. This was based on the theory that if it lies beyond the optimal limit, the output of a product or process with several characteristics was fully undesirable. At this juncture, it should be noted that "Minimum wear and Minimum Friction force" are the criteria for optimization. The minimization objective for wear and friction force was represented by Equations 7 and 8. The desirability objective functions for achieving minimum wear and minimum friction force are represented by d_2 and d_3 respectively. The composite desirability for the model is 0.9682.The desirability plot is shown in Figure 4. Optimal solution was shown in Table 5 using desirability function.

$$d_2 = \left(\frac{\text{wear}_{max} - \text{wear}}{\text{wear}_{max} - \text{wear}_{min}} \right) \tag{7}$$

$$d_3 = \left(\frac{\text{Frictionforce}_{max} - \text{frictionforce}}{\text{frictionforce}_{max} - \text{frictionforce}} \right) \tag{8}$$

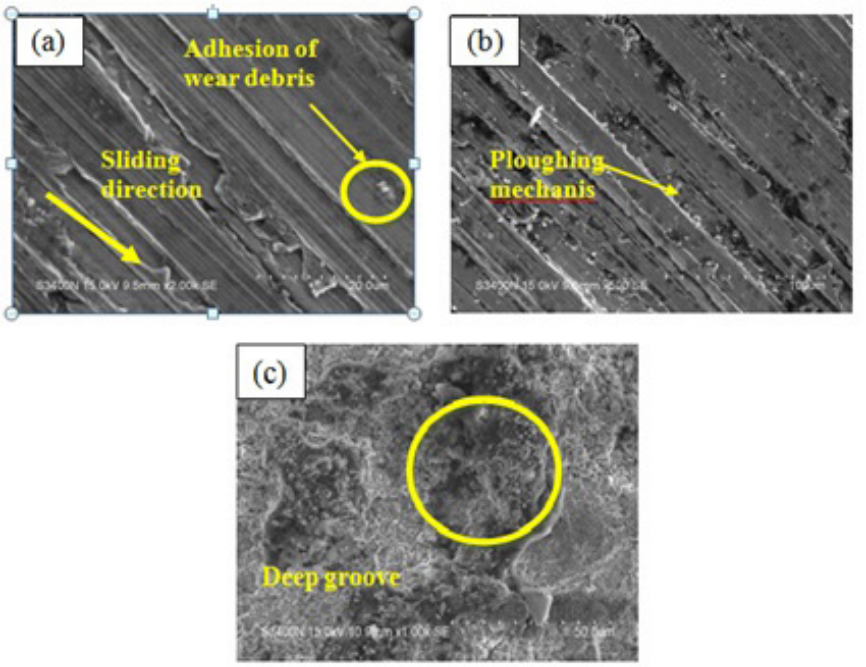

Figure 3. Shows the worn surface morphology of (a) Chromel – 6 wt.% TaC at 30N (b) Chromel – 3 wt.% TaC at 30N, and (c) Chromel – 0 wt.% TaC at 30N at higher magnification.

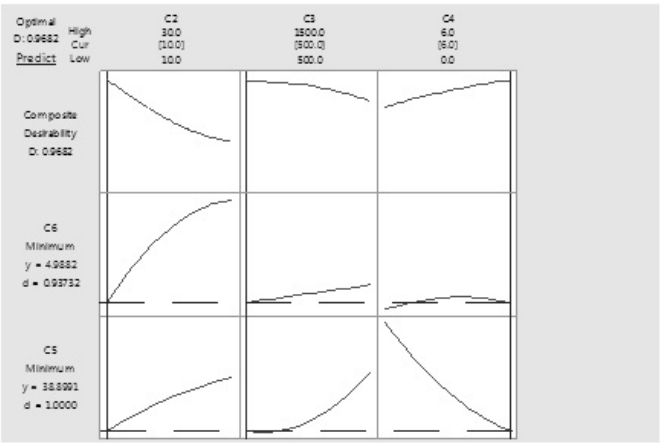

Figure 4. Desirability function.

Table 5. Optimal Solution using Desirability function.

Response	Goal	Target	Upper	Weight	Importance
Wear	Minimum	4.3	15.28	1	1
Friction Force	Minimum	40.8	109.7	1	1
Solution	C2	C3	C4		Desirability
1	10	500	6		0.968152

5. Conclusions

- Tantalum carbide based chromel composite was synthesized by stir casting route and its chemical composition was validated through EDAX.
- The wear behavior of synthesized chromel composite has been analyzed with different input process factors.
- Applied load, sliding distance and weight percentage were used as the essential factors to decide the outcomes, which are wear and frictional force.
- Response Surface Modeling (RSM) technique was used to find the optimal factors.
- Prediction of the wear and frictional force were done by developing the empirical model.
- The wear response factors and its effects were studied through contour plot.
- The maximum effect on wear was achieved at the weight percentage of 42.58%.
- The maximum effect on frictional force was attained at the applied load of 93.6%.
- The wear worn surface of chromel composite was observed through its microstructure.

6. References

1. Shabgard MR, Shotorbani RM. Mathematical modeling of machining parameters in electrical discharge machining of FW4 welded steel. World Acad Sci Eng Technol. 2009;53:403-9.
2. Baker CJ, Issac CA, Edwards D, Evans HT, Clayton R, van der Werf D, et al. Investigation of buffer gas trapping of positrons. J Phys B – At Mol Opt Phy. 2020;53(18):202-10.
3. Balan KN, Yashvanth U, Booma Devi P, Arvind T, Nelson H, Devarajan Y. Investigation on emission characteristics of alcohol biodiesel blended. Energy Sources A Recovery Util Environ Effects. 2019;41(15):1879-89.
4. Barabash P, Solomakha A, Sereda V. Experimental investigation of heat and mass transfer characteristics in direct contact exchanger. Int J Heat Mass Transfer. 2019;162:120-9.
5. Kim C, Gottstein G, Grummon DS. Plastic flow and dislocation structures in tantalum carbide: deformation at low and intermediate homologous temperatures. Acta Metall Mater. 1994;42:2291-301.
6. Liu L, Feng Y, Yu Z, Zhang Z. Microstructure and mechanical properties of spark plasma sintered TaC based ceramics. J Amer Soc.2010;93:2945-7.
7. Yu X-X, Weinberger CR, Thompson GB. An investigations of the phase stability in tantalum carbides. Acta Mater. 2014;80:341-9.
8. Peng J, Dong H, Hojamberdiev M, Yi D, Yang Y, Bao H, et al. Improving the mechanical properties of tantalum carbide particle-reinforced iron-based composite by varying the TaC contents. J Alloys Compd. 2017;726:896-905.
9. Ibrahim IA, Mohamed FA, Lavernia EJ. Particulate reinforced metal matrix composites: a review. J Mater Sci. 1991;26:1137-56.
10. Hashim J, Looney L, Hashmi MS. Particle distribution in cast metal matrix composites – Part I. J Mater Process Technol. 2002;123(2):251-7.
11. Saravanan S, Senthilkumar P, Ravichandran P. Mechanical, electrical, and corrosion behavior of AA6063/TiC composites synthesized via stir casting route. J Mater Res. 2017;32:606-14.
12. Goni J, Mitexelena I, Coleto J. Development of low coat metal matrix composites for commercial application. Mater Sci Technol. 2016;16(7-8):743-6.
13. Yu SY, Ishii H, Tohgo K, Cho YT, Diao D. Temperature dependence of sliding wear behavior in SiC whisker or SiC particulate reinforced 6061 aluminum alloy composite. Wear. 1997;213:21-8.
14. Singh G, Goyal S. Dry sliding wear behaviour of AA6082-T6/SiC/B4C hybrid metal matrix composites using response surface methodology. J Mater Des App.2016;1:1-13.
15. Sahoo P, Pal SK. Tribological performance optimization of electroless Ni–P coatings using the Taguchi Method and grey relational analysis. Tribol Lett. 2007;28(2):191-201.
16. Koksal S, Ficici F, Kayikci R, Savas O. Experimental optimization of dry sliding wear behavior of in situ AlB2/Al composite based on Taguchi's method. Mater Des. 2012;42:124-30.
17. Basavarajappa S, Chandramohan G, Paulo Davim J, Basavarajappa S, Chandramohan G. Application of Taguchi techniques to study dry sliding wear behaviour of metal matrix composites. Mater Des. 2007;28:1393-8.
18. Kaushik N, Singhal S. Wear conduct of aluminum matrix composites: a parametric strategy using Taguchi based GRA integrated with weight method. Cogent Eng.2018;5:1-17.
19. El Mahallawi A-K, Randa NA. Evaluation of effect of chromium on wear performance of high manganese steel. Mater Sci Technol. 2001;1:1385-90.
20. ASTM International. ASTM G-99-95. Standard test method for wear test with a pin on disc apparatus. West Conshohocken, PA: ASTM International; 1995.
21. Kandpal BC, Kumar J, Singh H. Optimization and characterization of EDM of AA 6061/10% Al2O3 AMMC using Taguchi's approach and utility concept. Prod Manuf Res. 2017;5(1):351-70.
22. Puneeth N, Satheesh J, Koti V, Koppad PG, Akbarpour MR, Naveen CJ. Application of Taguchi's method to study the effect of processing parameters of Al6082/B4C/Al2SiO5 hybrid composites on mechanical properties. Mater Res Express. 2019;6:1-10.
23. Kaviti RVP, Jeyasimman D, Parande G, Gupta M, Narayanasamy R, Koppad PG. Improving the friction and wear characteristics of AZ31 alloy with the addition of Al2O3 nanoparticles. Mater Res Express. 2019;6:101-10.
24. Lakshmikanthan A, Ram PT, Udayagiri SB, Koppad PG, Gupta M, Munishamaiah K, et al. The effect of heat treatment on the mechanical and tribological properties of dual size SiC reinforced A357 matrix composites. J Mater Res Technolo.2020;9:6434-52.
25. Mallikarjuna H, Siddaraju C, Kumar HS, Koppad P. Nanohardness and wear behavior of copper-SiC-CNTs nanocomposites. FME Transactions.2020;48(3):688-92.
26. Sethurama D, Keshavamurthy R, Paljor S, Rohit PE, Koppad PG. Effect of multiple reinforcements (CNT/Si3N4) on hardness, electrical conductivity and friction coefficient of aluminium hybrid composites. J Phys Conf Ser. 2020;1:1455-62.

27. Shivalingaiah K, Sridhar KS, Sethuram D, Shivananda Murthy KV, Koppad PG, Ramesh CS. HVOF sprayed Inconel 718/cubic boron nitride composite coatings: microstructure, microhardness and slurry erosive behavior. Mater Res Express. 2019;6:126-31.
28. Kumar A, Patnaik A, Bhat IK. Investigation of nickel metal powder on tribological and mechanical properties of Al-7075 alloy composites for gear materials. Powder Metall. 2017;60(5):371-83.
29. Walker JC, Rainforth WM, Jones H. Lubricated sliding wear behaviour of aluminium alloy composites. Wear. 2005;259:577-89.
30. Abbas A, Huang SJ, Ballóková B, Sülleiová K. Tribological effects of carbon nanotubes on magnesium alloy AZ31 and analyzing aging effects on CNTs/AZ31 composites fabricated by stir casting process. Tribol Int. 2020;142:105-10.
31. Huang SJ, Abbas A, Ballóková B. Effect of CNT on microstructure, dry sliding wear and compressive mechanical properties of AZ61 magnesium alloy. J Mater Res Technol.2019;8:4273-86.
32. Ballóková B, Falat L, Puchý V, Molčanová Z, Besterci M, Džunda R, et al. The influence of laser surface remelting on the tribological behavior of the ECAP-processed AZ61 Mg alloy and AZ61–Al2O3 metal matrix composite. Materials (Basel). 2020;13:2688-96.
33. Derringer S. Simultaneous optimization of several response variables. J Qual Technol. 1980;12:214-19.